

RESEARCH ARTICLE

The methyltransferase domain of the Respiratory Syncytial Virus L protein catalyzes cap N7 and 2'-O-methylation

Priscilla Sutto-Ortiz¹, Sergey Tcherniuk², Nina Ysebaert³, Pravien Abeywickrema³, Mathieu Noël⁴, Alice Decombe¹, Françoise Debart⁴, Jean-Jacques Vasseur⁴, Bruno Canard¹, Dirk Roymans³, Peter Rigaux³, Jean-François Eléouët², Etienne Decroly^{1*}

1 Aix Marseille Université, CNRS, AFMB UMR 7257, Marseille, France, **2** Unité de Virologie et Immunologie Moléculaires, INRAE, Université Paris Saclay, Jouy en Josas, France, **3** Janssen Infectious Diseases and Vaccines, Beerse, Belgium, **4** IBMM, Université de Montpellier, ENSCM, CNRS, UMR 5247, Montpellier, France

* etienne.decroly@univ-amu.fr



OPEN ACCESS

Citation: Sutto-Ortiz P, Tcherniuk S, Ysebaert N, Abeywickrema P, Noël M, Decombe A, et al. (2021) The methyltransferase domain of the Respiratory Syncytial Virus L protein catalyzes cap N7 and 2'-O-methylation. *PLoS Pathog* 17(5): e1009562. <https://doi.org/10.1371/journal.ppat.1009562>

Editor: Matthias Johannes Schnell, Thomas Jefferson University, UNITED STATES

Received: December 15, 2020

Accepted: April 15, 2021

Published: May 6, 2021

Copyright: © 2021 Sutto-Ortiz et al. This is an open access article distributed under the terms of the [Creative Commons Attribution License](https://creativecommons.org/licenses/by/4.0/), which permits unrestricted use, distribution, and reproduction in any medium, provided the original author and source are credited.

Data Availability Statement: All relevant data are within the manuscript and its [Supporting Information](#) files.

Funding: The research was funded by JANSSEN-CILAG S.A., a Company of Johnson & Johnson and the National Research Agency (ANR) under the program ANR DecRisP-cap (ANR-19_CE11_0017) awarded to JFE. The funding organization had no role in study design, data collection and analysis. P. R., N.Y., P.A. and D.R. are employees of Janssen Pharmaceutical Companies of Johnson & Johnson

Abstract

Respiratory syncytial virus (RSV) is a negative sense single-stranded RNA virus and one of the main causes of severe lower respiratory tract infections in infants and young children. RSV RNA replication/transcription and capping are ensured by the viral Large (L) protein. The L protein contains a polymerase domain associated with a polyribonucleotidyl transferase domain in its N-terminus, and a methyltransferase (MTase) domain followed by the C-terminal domain (CTD) enriched in basic amino acids at its C-terminus. The MTase-CTD of *Mononegavirales* forms a clamp to accommodate RNA that is subsequently methylated on the cap structure and depending on the virus, on internal positions. These enzymatic activities are essential for efficient viral mRNA translation into proteins, and to prevent the recognition of uncapped viral RNA by innate immunity sensors. In this work, we demonstrated that the MTase-CTD of RSV, as well as the full-length L protein in complex with phosphoprotein (P), catalyzes the N7- and 2'-O-methylation of the cap structure of a short RNA sequence that corresponds to the 5' end of viral mRNA. Using different experimental systems, we showed that the RSV MTase-CTD methylates the cap structure with a preference for N7-methylation as first reaction. However, we did not observe cap-independent internal methylation, as recently evidenced for the Ebola virus MTase. We also found that at μM concentrations, sinefungin, a S-adenosylmethionine analogue, inhibits the MTase activity of the RSV L protein and of the MTase-CTD domain. Altogether, these results suggest that the RSV MTase domain specifically recognizes viral RNA decorated by a cap structure and catalyzes its methylation, which is required for translation and innate immune system subversion.

and participated to the decision to publish and to the manuscript proofreading.

Competing interests: I have read the journal's policy and the authors of this manuscript have the following competing interests: P.R., N.Y., P.A, D.R are employees and possible shareholders of Janssen Pharmaceutical Companies of Johnson & Johnson.

Author summary

Respiratory syncytial virus (RSV) is responsible of infant bronchiolitis and severe lower respiratory tract infections in infants and young children, and the leading cause of hospitalization in children under one year of age. However, we still lack a vaccine and therapeutics against this important pathogen. The main enzymatic activities involved in RSV propagation are embedded in the Large (L) protein that contains the polymerase domain and also all the activities required for RNA cap structure synthesis and methylation. These post-transcriptional RNA modifications play a key role in virus replication because cap N7-methylation is required for viral RNA translation into proteins, and 2'-O-methylation hides viral RNA from innate immunity detection. Viral methyltransferase (MTase) activities are now considered potential antiviral targets because their inhibition might limit the virus production and strengthen early virus detection by innate immunity sensors. In this work, we compared the enzymatic activities of the MTase expressed as a single domain or in the context of the full-length L protein. We demonstrated that the MTase protein catalyzes the specific methylation of the cap structure at both N7- and 2'-O-positions, and we obtained the proof of concept that a S-adenosylmethionine analogue can inhibit the MTase activity of the L protein.

Introduction

Respiratory syncytial virus (RSV) is a major seasonal human pathogen that infects nearly all children before two years of age and is the leading cause of severe lower respiratory tract diseases in newborn and young children [1]. It is estimated that RSV infection causes more than 60,000 deaths per year in children younger than 5 years old, mostly in developing countries [2] (<http://perchresults.org>). In addition, RSV is also recognized as a significant cause of severe respiratory infections in the elderly and high-risk adults [3]. Currently, the only clinical intervention is passive prophylaxis with the humanized monoclonal antibody palivizumab, used as a treatment to prevent hospitalization and severe RSV infections in high-risk populations [4]. Nevertheless, its use is restricted due to its high cost and modest efficacy [5]. Therefore, urgent efforts are needed to develop therapeutic agents against RSV infections, such as the small-molecule inhibitors currently in development to target the fusion process [6], or antiviral compounds against the replication/transcription machinery that is essential for viral propagation.

RSV is a filamentous enveloped, non-segmented negative-sense (NNS), single-stranded RNA virus that belongs to the *Orthopneumovirus* genus, *Pneumoviridae* family, *Mononegavirales* order. This family also includes the human metapneumovirus (hMPV) that belongs to the *Metapneumovirus* genus and is another leading cause of acute respiratory infections in children. The *Mononegavirales* order comprises other important pathogens and sometimes deadly viruses, such as rabies and Ebola viruses [7].

The 15.2 kb RSV genome contains 10 genes that encode 11 proteins [6]. Three viral proteins are essential for RSV genome replication: the nucleoprotein (N), the large protein (L), and the phosphoprotein (P) [8,9]. The M2-1 protein is essential for viral transcription [10]. The N protein associates with viral RNA to protect it from cellular nucleases and recognition by the innate immune system [11,12]. The 250 kDa L protein harbors three conserved enzymatic domains: the RNA-dependent RNA polymerase (RdRp) domain, the polyribonucleotidyltransferase (PRNTase or capping domain), and the methyltransferase (MTase) domain. The MTase domain is followed by the C-terminal domain (CTD), which is the most variable domain in NNS viruses. Despite the lack of obvious primary sequence conservation, it has

been suggested that this domain, which is enriched in basic amino acids, forms a clamp with the MTase domain that allows the recognition of the RNA substrate for methylation [13]. Thus, the L protein of *Mononegavirales* participates in viral RNA synthesis, and also ensures its capping and methylation as well as the addition of the poly-A tail at the 3' end of each transcript. The P protein, the main cofactor of the L polymerase, allows its interaction with the nucleoprotein-RNA complex [8,9,14,15]. mRNA capping and methylation are important co-transcriptional events during viral RNA biogenesis. The cap structure consists of a 7-methylguanosine (m^7G) moiety linked to the first nucleotide of the transcript via a 5'-5' triphosphate bridge [16]. The cap structure found at the 5' end of eukaryotic mRNAs has several important biological roles. For host cells mRNA, this modification i) ensures the protection of mRNA from degradation by 5'-3' exoribonucleases; ii) allows mRNA translation by ensuring its efficient recognition by the eukaryotic translation initiation factor 4E (eIF4E) [17,18]; iii) directs pre-mRNA splicing and host mRNA export from the nucleus [19]; and iv) allows if missing, the recognition of foreign RNAs (including viral transcripts) as 'non-self' by recognition receptors, such as retinoic-acid inducible gene (RIG)-I [20–22]. In view of the pleiotropic role played by the RNA cap structure during infection, RNA capping enzymes and MTases are now considered as promising targets for the development of highly specific antiviral drugs [23,24]. Accordingly, mutation of MTase catalytic residues and molecules that block the cap MTase activity induce a strong antiviral response [25,26] and limit viral mRNA translation [24,27] in different viral families.

The multifunctional L proteins of *Mononegavirales* have evolved independently from other known eukaryotic cap-synthesizing enzymes [28–30], and use an unconventional mechanism for mRNA cap synthesis that has been so far, only assessed for VSV [31,32] (Fig 1).

Conversely, MTase activities have been characterized in a larger set of mononegaviruses, including VSV [27], Ebolavirus [13,33] and hMPV [34]. The studies on the Ebola Sudan virus (SUDV) MTase and hMPV MTase revealed cap-dependent and cap-independent methyltransferase activities. For the SUDV MTase, a cap-independent 2'-O-MTase activity that targets internal adenosine residues was also described [33]. Recently, the 3.2-Å cryo-EM structure of RSV L bound to tetrameric P was described providing the first structural characterization of a viral phosphoprotein in complex with a viral L protein [35]. The structure reveals a striking tentacular arrangement of P, with each of the four monomers adopting a distinct conformation as it interacts with specific regions on L. In addition, the study provides the first structural information for the RdRp and capping domains of RSV L. However, the MTase and C-terminal domains of L protein are not visible in the cryo-EM map suggesting that the enzymatic activity of the RSV MTase can be regulated in the context of the full-length L-P protein complex. Although the structure of the RSV L protein in complex with P [35] as well as that of VSV [36,37] have brought important insights into the structure-function relation in the RSV RNA genome transcription and replication, the mechanism and the order of the reactions governing mRNA cap methylation are still elusive for viruses belonging to this family.

In this study, we expressed a 412-residue fragment of the RSV L protein that includes the MTase domain and the CTD (MTase-CTD) in bacteria. We found that the purified recombinant RSV MTase-CTD protein sequentially methylates the N7 and 2'-O positions of capped synthetic RNAs that mimic the RSV mRNA 5' end sequence. We observed similar enzymatic activities with purified full-length L protein co-expressed with P. However, we did not detect any internal methylation using capped and uncapped RNAs with both constructs. These findings suggest that the RSV MTase is a strict cap-dependent MTase.

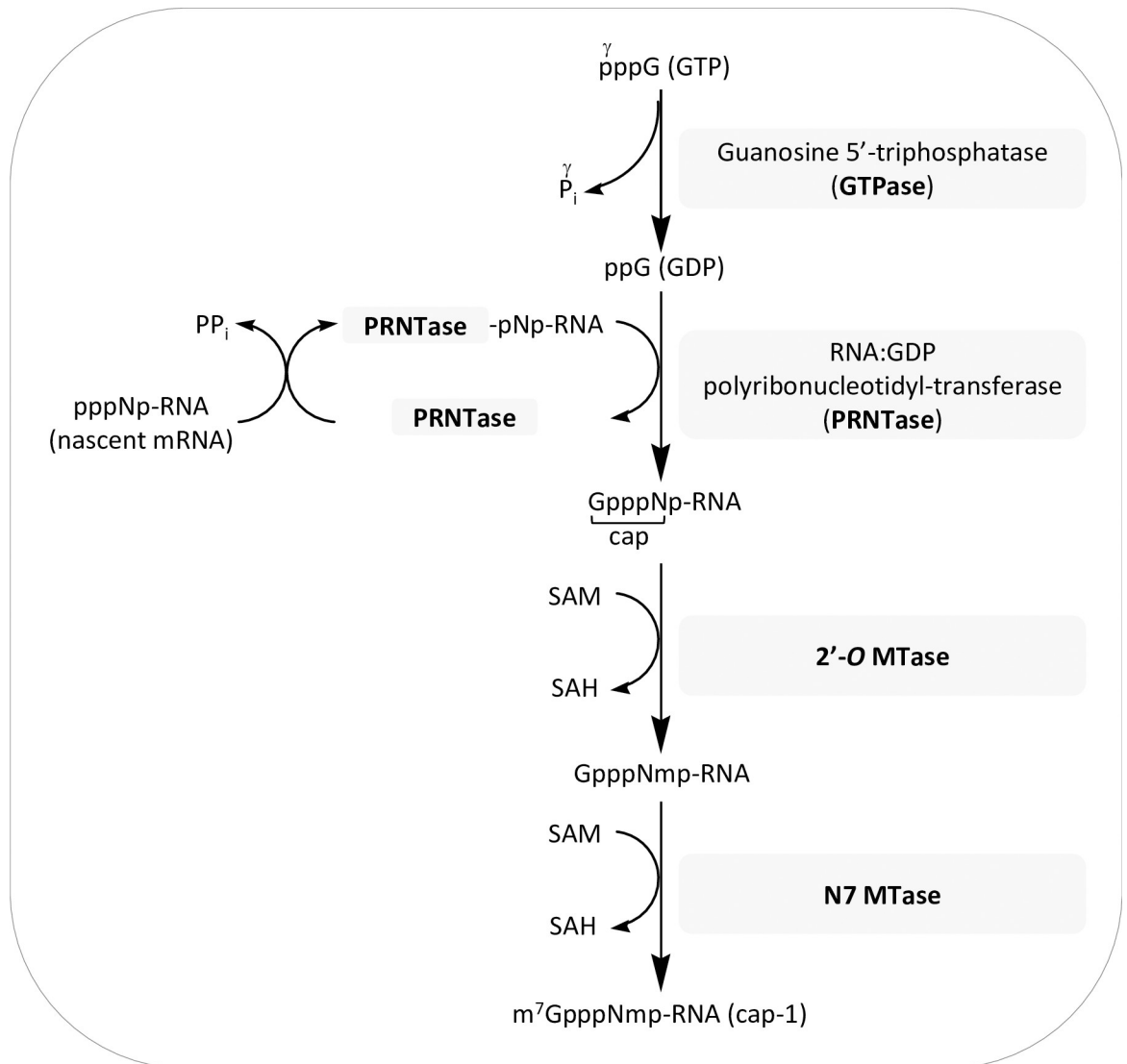


Fig 1. Schematic representation of the unconventional mechanism of mRNA cap formation by VSV L Protein. Possible mechanism described for the vesicular stomatitis virus (VSV) L protein where first hydrolyzes the γ -phosphate of guanosine-5'-triphosphate (GTP; Gppp) to yield guanosine diphosphate (GDP; Gpp) and inorganic phosphate (P_i) [31]. Then, nascent mRNA transcripts that carry a triphosphate group at their 5' end form a covalent adduct with the PRNTase histidine residue present in the conserved 'HR' motif of L, releasing pyrophosphate (PP_i). The transfer of pNp-RNA to the GDP (in which N denotes the first transcribed nucleotide) forms the capped structure (GpppNp-RNA) that is subsequently methylated by S-adenosyl-L-methionine (AdoMet or SAM)-dependent methyltransferases (MTases) present in the C-terminal domain of L. First, the (nucleoside-2'-O)-methyltransferase (2'-O-MTase) transfers the methyl group from SAM to the first nucleotide of the nascent RNA, forming GpppNmp-RNA and releasing S-adenosyl homocysteine (SAH). Then, the cap structure is methylated on the guanine N7 position by the (guanine-N7-) methyltransferase (N7-MTase) to generate cap-1 RNA (m^7 GpppNmp-RNA).

<https://doi.org/10.1371/journal.ppat.1009562.g001>

Results

Cap-dependent MTase activity of RSV MTase-CTD

Based on the alignment of *Mononegavirales* MTases (Figs 2A and S1), we designed the RSV MTase-CTD construct that spans amino acids 1755 to 2165 and includes a 6 His-tag at the N-terminus. This construct corresponds to the MTase domain that includes the conserved K-D-K-E catalytic tetrad and the SAM/SAH binding GxGxGx motif, followed by the CTD

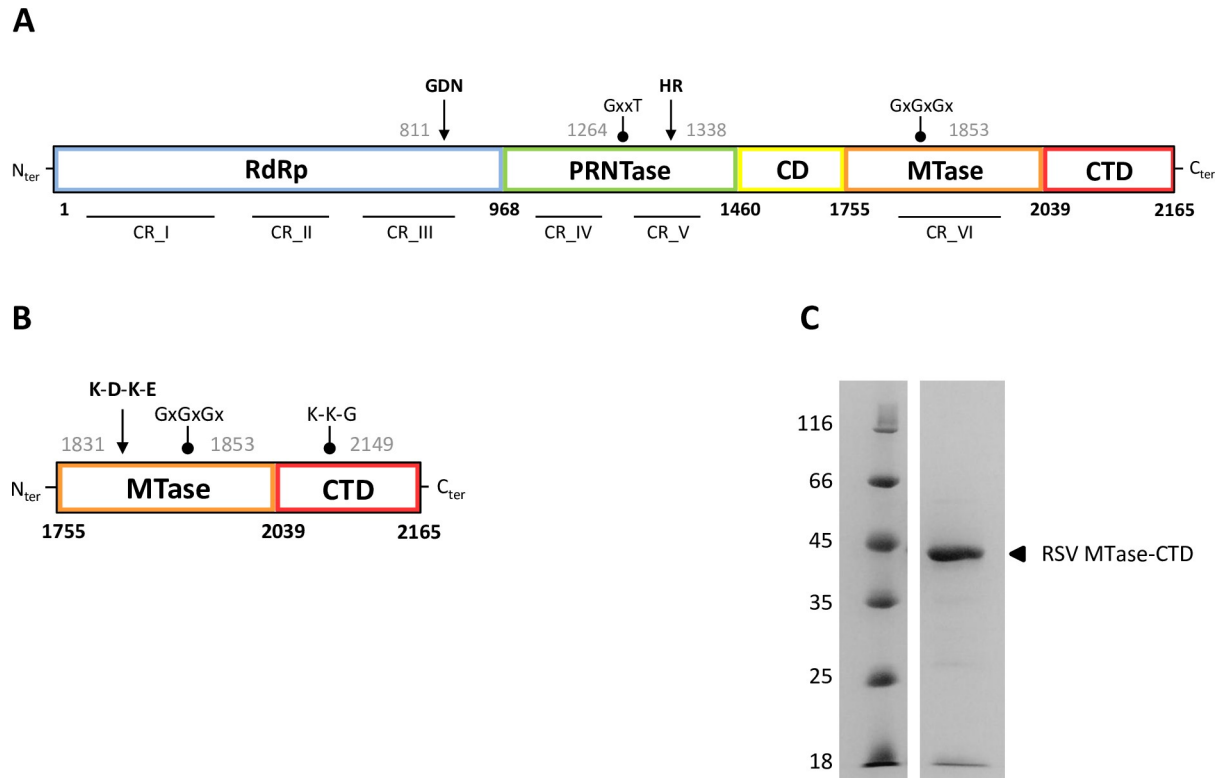


Fig 2. The recombinant RSV MTase-CTD protein. (A) Schematic representation of the domain organization of the RSV L protein. Blue, RNA-dependent RNA-polymerase (RdRp) domain; green, polyribonucleotidyl-transferase (PRNTase) domain; yellow, connector domain (CD); orange, methyltransferase (MTase) domain; red, C-terminal domain (CTD). Amino acid residue numbers indicate the functional domain boundaries. The conserved regions (CR) within the L proteins of non-segmented negative-strand RNA viruses are indicated. Arrows denote the position of active site residues required for function, and dots indicate conserved motifs with the starting amino acid residue number in gray. (B) The RSV MTase-CTD fragment was defined based on the alignment with the VSV L protein. Arrow indicates the K₁₈₃₁-D₁₉₃₆-K₁₉₇₃-E₂₀₀₄ catalytic tetrad, typical of 2'-O-MTases. Dots indicate conserved motifs with the starting amino acid residue number in gray: the GxGxGx SAM/SAH binding site motif in the MTase domain, and the K-K-G motif, reminiscent of eukaryotic GTases, in the CTD domain. (C) SDS-PAGE of the purified recombinant RSV MTase-CTD protein containing an N-terminal histidine tag (49.3 kDa). Molecular weights (in kilodaltons) of the ladder are shown on the left, and the MTase-CTD band is labeled on the right.

<https://doi.org/10.1371/journal.ppat.1009562.g002>

required for substrate binding (Fig 2B). After expression in bacteria, we purified the recombinant RSV MTase-CTD protein to homogeneity by two steps of affinity chromatography followed by size-exclusion chromatography. SDS-PAGE analysis of the purified MTase-CTD protein (expected molecular weight of 49.3 kDa) showed a band of \approx 45 kDa after Coomassie blue staining (Fig 2C). Matrix-Assisted Laser Desorption/Ionization Time-of-Flight (MALDI-TOF) analysis of the protein band confirmed its identity. We then assessed its MTase activity (optimum pH and the influence of Mg²⁺ ions) by incubating the purified MTase-CTD protein with a short-capped RNA substrate (GpppG-RSV₉), in the presence of a radiolabeled methyl donor (³H-SAM). After separation of the radiolabeled capped RNAs from ³H-SAM by filter-binding assay (FBA), we determined the enzymatic activity by counting the radioactivity transferred to the RNA template. The MTase reaction showed a bell-shaped pH profile with an activity peak between pH 7.0 and 7.5 (S2A Fig). The RSV MTase-CTD activity was barely influenced by addition of 0.5 mM Mg²⁺ ions, and was only slightly decreased in the presence of 5 mM Mg²⁺ (S2B Fig).

We next determined the MTase-CTD substrate length preference by monitoring the transfer of the ³H-methyl group from SAM molecules to synthetic capped RNAs of increasing

lengths (5-, 9-, 11- and 15- nucleotides) that correspond to the 5' end of RSV mRNA. As the purified RSV MTase-CTD showed a dose-response MTase activity, for these experiments we used 25 nM of recombinant protein because the activity was detectable even at this low concentration. These experiments showed that the RSV MTase-CTD efficiently methylated the capped RNAs that mimic the 5' end of RSV L mRNA [38], with preference for 11-nucleotide-long RNA (Fig 3A). We also evaluated its MTase activity on 9-nucleotide-long RSV₉ RNA harboring a 5' end cap-1 structure (^mGpppG_m) and on uncapped RNAs (pppG_m, pppG). The RSV MTase-CTD exhibited cap-dependent methyltransferase activity, because GpppG-RSV₉ was efficiently methylated, but not ^mGpppG_m-RSV₉ (Fig 3B). Moreover, the RSV MTase-CTD protein did not methylate uncapped RNA substrates (pppG_m-RSV₉, pppG-RSV₉), suggesting that the RSV MTase is a cap-dependent MTase. Finally, concerning the internal methylation activity, we observed that in our experimental conditions, the ^mGpppG_m-RSV₉ RNA substrate and homopolymeric 27-mer RNAs (A₂₇, G₂₇, C₂₇, U₂₇) (Fig 3C) were barely methylated. Altogether, our results suggest that the RSV MTase catalyzes the cap structure methylation, and is scarcely involved in the internal RNA methylation activity.

We then analyzed the substrate-sequence specificity using various synthetic capped RNAs with different viral 5' end sequences (Fig 4). The RSV MTase-CTD displayed some sequence specificity, because it was mainly active on RSV₉, RSV₁₁ 3G and hMPV₉ RNAs that share a GGG sequence at their 5' end. Moreover, its MTase activity was 10 times lower in the presence of RSV sequences that contain four G nucleotides (RSV₁₁ 4G) and mimic the 5' end of the RSV P and N mRNAs [39,40]. Similarly, MTase-CTD was poorly active on RNA sequences that mimic the 5' end of other viral genomes. Nevertheless, the MTase activity was slightly higher with substrates starting with Gppp G (SUDV₁₃, MERS₁₃) compared with Gppp AG (WNV₁₃, DV₁₃) and particularly Gppp AA (RABV₁₃) or Gppp AU (SARS-CoV₁₀).

To further characterize the RSV MTase activity, we mutated some conserved residues of the MTase catalytic site, in the SAM-binding site, and some basic residues supposed to participate in RNA binding (S1A Fig). After affinity chromatography purification, some variants were not expressed or were insoluble, particularly those harboring the K1831A, K1973A, K1999A, G1853S, G1857S, and L1878A substitutions. On the other hand, the MTase mutants that were successfully expressed and purified (S1B Fig) showed the expected molecular weight after SDS-PAGE analysis. The MTase activity of the RSV MTase-CTD protein was almost abolished by the D1936A and E2004A substitutions within the K-D-K-E tetrad (S1C Fig). This demonstrated that the catalytic tetrad is essential for the MTase activity. Serine substitution of G residue (G1855S) in the GxGxGx SAM/SAH binding-site motif and alanine substitution of residues R1820A, E1938A and S1998A involved in RNA-binding also strongly inhibited the MTase activity of the RSV MTase-CTD.

The RSV MTase-CTD catalyzes N7- and 2'-O-methylation of the RNA cap structure

To further characterize the methylation catalyzed by the RSV MTase-CTD, we compared the MTase activity on synthetic 9-mer RSV₉ RNAs with different cap structures (GpppG, ^mGpppG, GpppG_m and ^mGpppG_m). Compared with the GpppG-RSV₉ RNA (Fig 5A), the RSV MTase-CTD methylation activity was reduced by ~50% in the presence of the RNAs with the monomethylated ^mGpppG-RSV₉ and GpppG_m-RSV₉ cap structures, and was not detectable when both the N7 and 2'-O positions of the cap were methylated (^mGpppG_m-RSV₉). This suggested that the RSV MTase-CTD protein catalyzes N7 and 2'-O-methylation of the cap structure. We then determined the optimum pH of each MTase activity by measuring the transfer of the ³H-methyl group from SAM molecules to the GpppG_m-RSV₉ and ^mGpppG-RSV₉

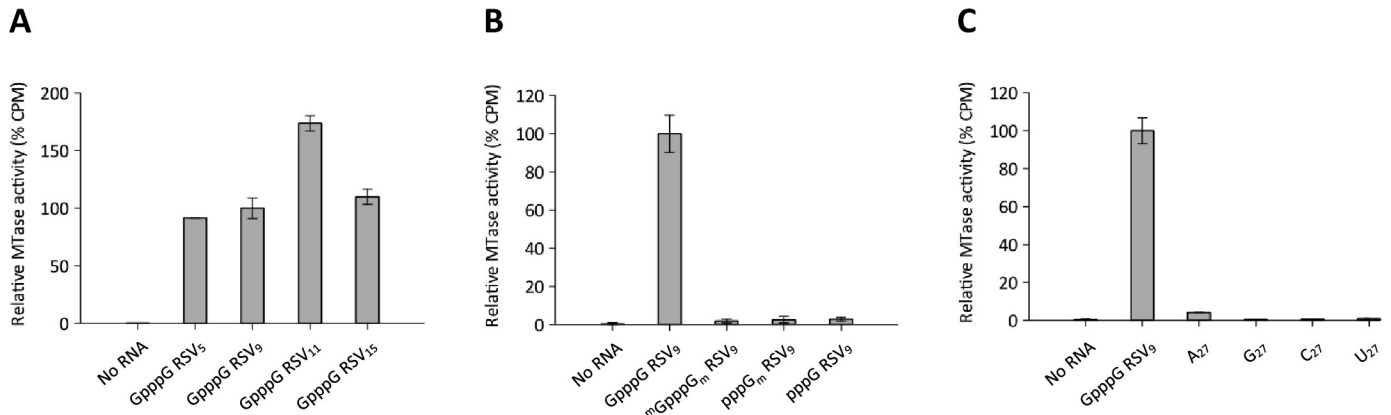


Fig 3. Cap-dependent MTase activity of the recombinant RSV MTase-CTD protein. (A) The transfer of tritiated methyl groups from S-adenosylmethionine (SAM) molecules to synthetic capped RNAs of different lengths (5-, 9-, 11- and 15- nucleotide-long), which mimic the 5' end of RSV mRNA, was assessed by filter-binding assay. The RSV MTase-CTD was used at the concentration of 25 nM. Data are the mean values ± standard error of the mean (SEM) of three independent measurements. (B) MTase activity measurements using capped and uncapped RSV₉ RNAs (GGG ACA AAA) methylated at specific positions. Values represent the mean ± SEM (n = 3). (C) MTase activity evaluation on synthetic, 27-nucleotide-long homopolymeric RNAs (HO-(G/C/U/A)₂₇). Values were normalized to the activity on Gppp GGG-RSV₉, and are the mean ± SEM (n = 3). CPM, count per minute.

<https://doi.org/10.1371/journal.ppat.1009562.g003>

substrates. The curves adopt a bell-shaped profile with an optimum at pH 7 to 7.5 for the N7-MTase activity and a broader pH range from pH 7 to 8 for the 2'-O-MTase activity (Fig 5B).

We next confirmed by thin-layer chromatography (TLC) the nature of the methylations catalyzed on the RSV₉ RNA cap structure. To this aim, pppG-RSV₉ RNA was incubated with the vaccinia virus GTase/N7-MTase capping system in the presence of [α -³²P]-GTP and SAM in the reaction buffer, to produce GpppG-RSV₉ or ^mGpppG-RSV₉. A time-course experiment was then performed using the GpppG-RSV₉ RNA as substrate and the RSV MTase-CTD protein. We digested the reaction products with P1 nuclease before TLC analysis of the cap

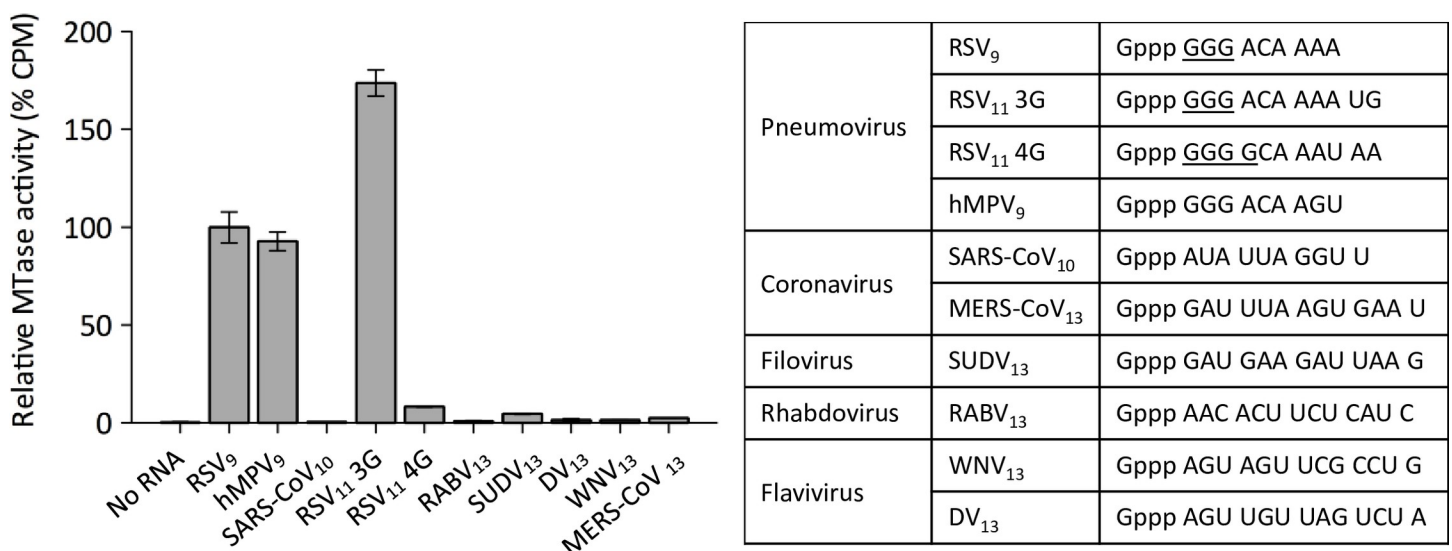


Fig 4. RSV MTase activity is sequence-specific. Substrate specificity was determined by filter-binding assay, using the synthetic capped RNA substrates with different 5' end sequences and lengths (numbers after virus abbreviation) described in the table on the right. hMPV, human Metapneumovirus; SARS-CoV, Severe Acute Respiratory Syndrome Coronavirus; MERS, Middle East Respiratory Syndrome; SUDV, Sudan Ebolavirus; RABV, Rabies virus; WNV, West Nile virus; DV, Dengue virus. The RSV MTase-CTD was used at 25 nM. Values were normalized to the activity on Gppp GGG RSV₉, and are the mean ± SEM (n = 3).

<https://doi.org/10.1371/journal.ppat.1009562.g004>

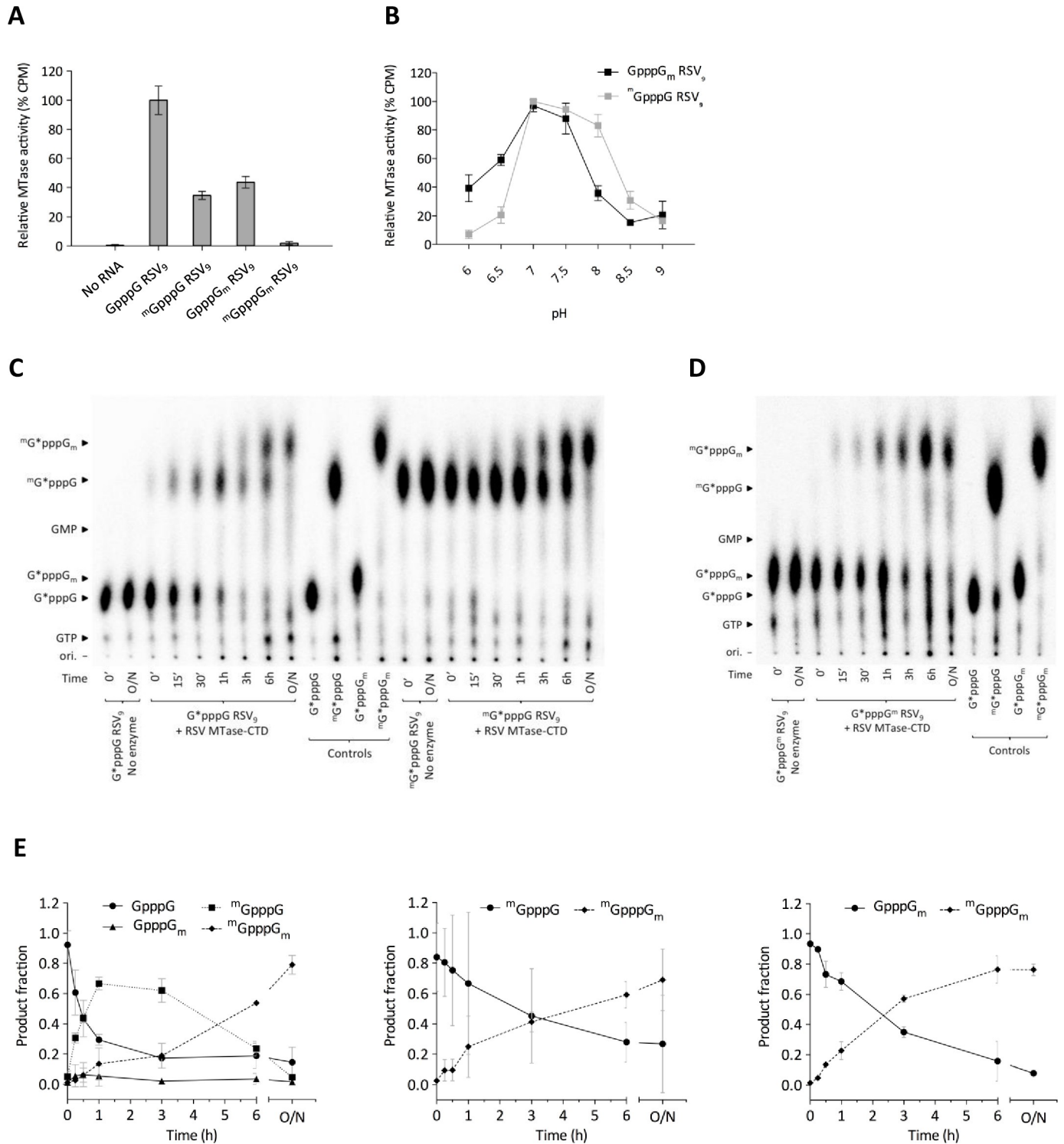


Fig 5. N7- and 2'-O-methylation activity of the RSV MTase-CTD protein. (A) MTase activity measurements by filter-binding assay using capped RSV₉ RNAs (GGG ACA AAA). Values were normalized to the activity on Gppp GGG-RSV₉ and are the mean ± SEM (n = 3). (B) Time-course of N7- and 2'-O-methylation activities on GpppG_m and ^mGpppG RSV₉ RNAs, respectively, by the RSV MTase-CTD protein (25 nM) measured by filter-binding assay at different pH (from 6.0 to 9.0). The plotted values were obtained after 3 h incubation at 30°C. Values were normalized to the maximum activity on each substrate and are the mean ± SEM (n = 3). (C, D) Thin-layer chromatography analysis of cap structures of control RNAs and substrates (G*pppG (C left), ^mG*pppG (C right), G*pppG_m (D)) incubated with the RSV MTase-CTD (* indicates G(³²P)-labeled). Nucleotides 2–9 were removed by nuclease P1 digestion and caps were separated using 0.65 M LiCl as mobile phase. Controls (G*pppG, G*pppG_m, ^mG*pppG, ^mG*pppG_m) were obtained using the pppG-RSV₉ substrate and vaccinia virus MTases that

specifically methylate caps at the N7 or 2'-O positions. The RSV MTase-CTD was used at the concentration of 25 nM. O/N:overnight. (E) Densitometry quantitations of TLC analysis expressed as a ratio of the substrate consumption (G^*pppG (left), ${}^mG^*pppG$ (middle), G^*pppG_m (right)) and product formation over time. Values are the mean \pm SEM ($n = 3$).

<https://doi.org/10.1371/journal.ppat.1009562.g005>

structure. After 15 min, $GpppG-RSV_9$ was converted into ${}^mGpppG-RSV_9$ ($30.7\pm 4.7\%$) or $GpppG_m-RSV_9$, ($1.5\pm 0.5\%$) (Fig 5C left). After a longer incubation period, we could detect the double methylated product (mGpppG_m), and the products corresponding to the monomethylated cap structures (mGpppG and $GpppG_m$) disappeared progressively, as expected. After 6 hours of incubation, $GpppG-RSV_9$ was almost entirely converted into ${}^mGpppG_m-RSV_9$. Similarly, when we used the ${}^mGpppG-RSV_9$ RNA substrate (Fig 5C right) or $GpppG_m-RSV_9$ RNA (Fig 5D), we detected the mGpppG_m product after 15 min of reaction, demonstrating that in our experimental conditions, the 2'-O-methylation can occur after N7 methylation of the guanosine residue of the cap structure.

In order to estimate kinetic parameters of the cap methylation process, time-course assays were performed in triplicates, and we quantified by densitometry the substrate and the methylated species detected on TLC. The quantification shows that when the MTase-CTD protein is incubated with $GpppG-RSV_9$ substrate (Fig 5E left), the estimated initial velocities (V_i) for the generation of ${}^mGpppG-RSV_9$ or $GpppG_m-RSV_9$ product are $V_i = 0.948\pm 0.119$ and $V_i = 0.078\pm 0.026$ product formation/h, respectively. The N7 methylation is about 12 fold faster than the 2'-O methylation in our experimental conditions. The subsequent 2'-O methylation of ${}^mGpppG-RSV_9$ then takes place resulting in the ${}^mGpppG_m-RSV_9$ product for which we obtained a $V_i = 0.132\pm 0.007$ product formation/h. In addition, the V_i estimated for the generation of ${}^mGpppG_m-RSV_9$ product from either ${}^mGpppG-RSV_9$ (Fig 5E middle) or $GpppG_m-RSV_9$ (Fig 5E right) substrate provides a similar value of $V_i = 0.256\pm 0.025$ and $V_i = 0.234\pm 0.013$ product formation/h, respectively. Altogether our results suggest that the cap methylation by the RSV MTase-CTD occurred at the N7 and also 2'-O positions, with a preference for N7 methylation as first reaction step. In addition it is likely that the 2'-O methylation is the limiting step for the capping reaction carried out by the MTase-CTD protein.

The MTase domain and the RSV L-P complex display similar N7 and 2'-O-MTase activities

Cryo-EM studies indicate that the MTase domain of L protein can accommodate different positions, suggesting that its enzymatic activity can be regulated in the context of the full-length L protein or in the L-P protein complex [35]. To further characterize the MTase activities of the purified L-P complex (Fig 6A), we analyzed the nature of the cap structure methylation by TLC analysis. In this time-course experiment, we incubated RNAs carrying different types of ${}^{32}P$ -radiolabeled cap structures with the RSV L-P complex, and then digested the reaction products with P1 nuclease. TLC analysis of the released cap structures methylated at position N7 (cap-0), 2'-O, or both (cap-1) showed that the RSV L-P complex methylated $GpppG-RSV_9$ at the N7 position, as indicated by the presence of ${}^mGpppG-RSV_9$ after 30 min of reaction (Fig 6B left). However, after 6 hours incubation, we could barely detect the double methylated ${}^mGpppG_m-RSV_9$ product. We obtained similar results when we incubated the RSV L-P complex with the ${}^mGpppG-RSV_9$ (Fig 6B right) or $GpppG_m-RSV_9$ substrates, suggesting that 2'-O-methylation is a limiting step in our experimental conditions. After overnight incubation of the reaction mixtures, we could observe a faint band corresponding to the mGpppG_m cap structure, indicating that 2'-O-methylation occurs (Fig 6C), but that its kinetics were slower when using the L-P complex than the RSV MTase-CTD alone. These results indicate that the RSV MTase in the context of the L-P complex catalyzes more efficiently N7 methylation of

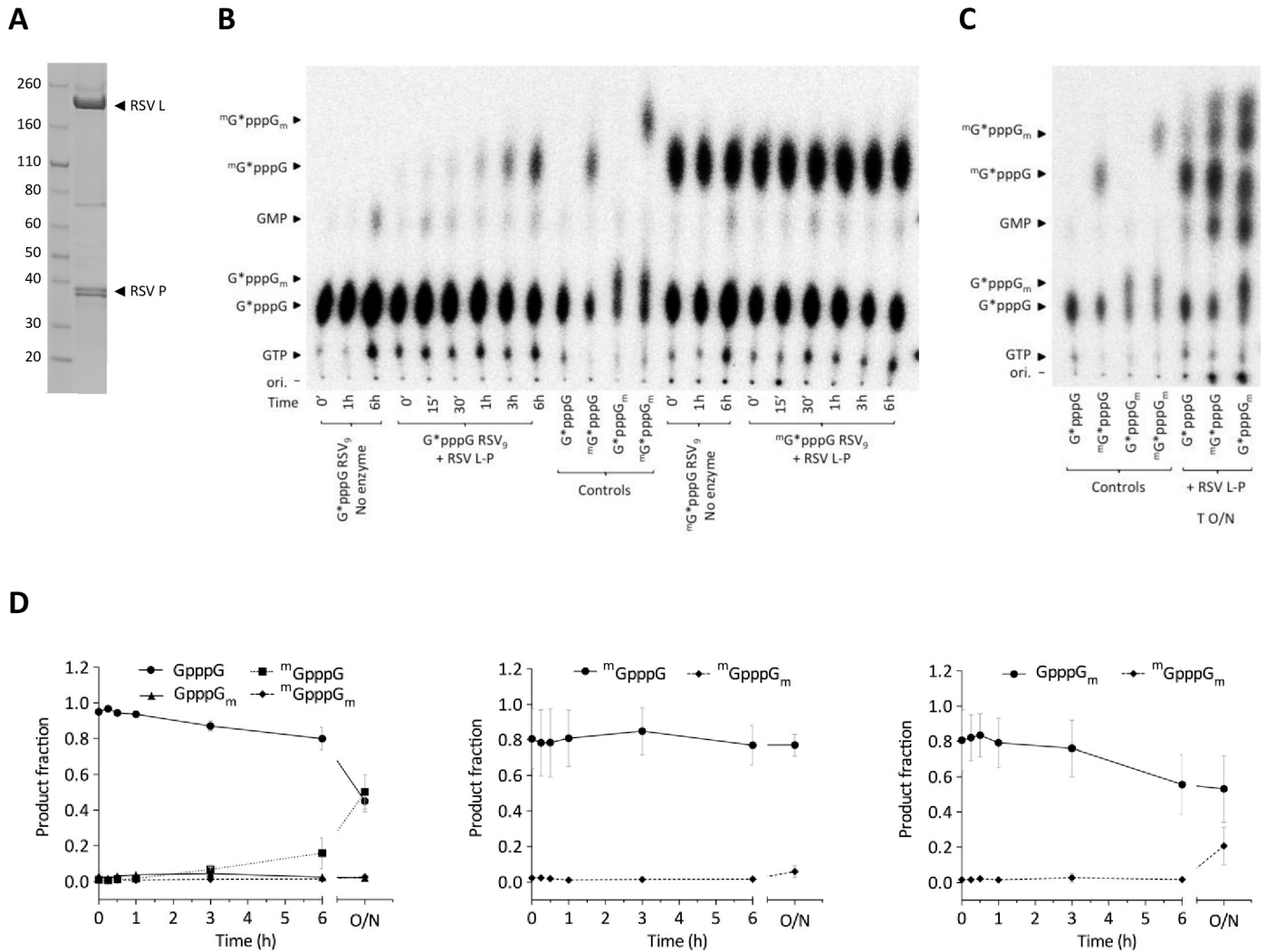


Fig 6. MTase activity of the RSV L-P complex. (A) SDS-PAGE of the purified RSV L-P complex. Molecular weights (in kilodaltons) of the ladder are shown on the left, and the L and P bands are labeled on the right. (B) Time-course analysis of methylation by thin-layer chromatography of the cap structures of control RNAs and substrates (G^*pppG and m^*G^*pppG) incubated with RSV L-P (* indicates $G^{(32}P)$ -labeled) for up to 6 h at 30°C. (C) After overnight (O/N) incubation, nucleotides 2–9 were removed by nuclease P1 digestion and caps were separated using 0.65 M LiCl as mobile phase. Controls (G^*pppG , G^*pppG_m , m^*G^*pppG , $m^*G^*pppG_m$) were obtained using the pppG-RSV₉ substrate and vaccinia virus MTases that specifically methylate caps at the N7 or 2'-O positions. The RSV L-P complex was used at the concentration of 100 nM. (D) Densitometry quantifications of TLC analysis expressed as a ratio of the substrate consumption (G^*pppG (left), m^*G^*pppG (middle), G^*pppG_m (right)) and product formation over time. Values are the mean \pm SEM (n = 3).

<https://doi.org/10.1371/journal.ppat.1009562.g006>

capped RNA than 2'-O-methylation. These observations were confirmed by the densitometry quantitation of the TLC analysis (Fig 6D), but the kinetic parameters were not determined due to the low amount of reaction product detected in our experimental conditions.

RSV MTase inhibition by SAM and Cap analogues

As the RSV MTase uses SAM as methyl donor to catalyze cap N7 and 2'-O-methylation, we wondered whether SAM or cap analogues could competitively inhibit the RSV MTase enzymatic activity. We first determined whether cap analogues inhibit the RSV MTase activity. We incubated N7-methylated (m^*GpppA , m^*GDP) and unmethylated ($GpppA$, $GpppG$) cap analogues with the RSV MTase-CTD, and determined the methylation of G^*pppG -RSV₉-RNA by

FBA as previously described. The cap analogue GpppG at 50 μM inhibited by 50% the activity of the RSV MTase-CTD (S3A Fig), whereas the GpppA (S3A Fig) and the N7-methylated cap analogues (S3B Fig) showed lower inhibitory activity.

We next measured by FBA the inhibition of the MTase activity by SAM/SAH by performing a dose-response assay using increasing concentrations of sinefungin and SAH (the methylation reaction by-product). After activity normalization (typical dose-response inhibition curve in Fig 7), deduction of the half-maximal inhibitory concentration (IC_{50}) by Hill slope curve-fitting [equation: $Y = 100/(1+((X/\text{IC}_{50})^{\text{Hillslope}}))$] showed IC_{50} values of 6.4 μM and 24.7 μM for sinefungin and SAH, respectively. To confirm the robustness of the enzymatic assay performed with the RSV MTase-CTD protein, we also carried out a dose-response inhibition assay using the RSV L-P complex in the presence of sinefungin and SAH. The IC_{50} values were in the same range (9.8 μM and 37.8 μM for sinefungin and SAH, respectively), confirming that the MTase domain can be inhibited by SAM analogues, which opens promising perspectives for the development of high-throughput screening assays to identify new antiviral compounds. However, antiviral activity with sinefungin performed in cellular assay did not show inhibition activity on replication of RSV in HeLa cells before toxicity. Of note, the antiviral activity of sinefungin has been shown to inhibit VSV replication in BHK cells using plaque assay, with a half maximal effective concentration (EC_{50}) of 220 μM [41].

Discussion

Mononegaviruses share a similar genetic organization in which the L protein orchestrates the replication/transcription and capping activities. However, the MTase activity specificity might vary according to the virus family. Indeed, it was shown that the Ebola virus MTase catalyzes internal methylation of RNA in addition to cap methylation, whereas the hMPV MTase mainly catalyzes N7 and 2'-O-methylation of the cap structure present at the 5' end of viral RNA [33,34]. So far, descriptions in the literature involving the activity of RSV L have been assessed as independent structural fragments of the polymerase with dimerization tags resulting in trans-complementation of RdRp bioactivity [42]. Nevertheless, to date, information on RSV RNA methylation mechanisms is missing. In this work, we produced and purified the soluble RSV MTase-CTD protein, and we analyzed *in vitro* its enzymatic activity using different RNA substrates. We found that the RSV MTase-CTD is active at 25 nM, unlike the MTase domain purified from other NNS viruses, such as Ebola virus [33] or hMPV [34], that are active at μM concentrations. The difference in the amount of protein required for MTase activity determination could be explained by the fact that Ebola virus [33] and hMPV MTases [34] were purified using astringent conditions (*i.e.* arginine) to ensure their solubility, whereas the RSV MTase-CTD was purified under mild conditions that are probably more favorable for MTase activity assay. Mutagenesis studies demonstrated that the RSV MTase activity is specific and is strongly impaired by single alanine substitution of residues belonging to the catalytic site (K-D-K-E), as well as mutation of conserved residues that are thought to participate in SAM or RNA-binding. Similar mutation effects were previously described for the Ebola SUDV [33] and hMPV [34] MTases.

We observed that the RSV MTase displays sequence preference because the protein methylates more efficiently capped RNA starting with GGG, a sequence that is present at the 5' end of most RSV mRNAs [39]. Conversely, we did not detect any obvious effect of RNA length (fragments between 5 and 15 nucleotides in length were tested). Moreover, the presence of a fourth G at the 5' end of RNA reduced the MTase activity. This was unexpected because some RSV mRNAs (from P and N proteins) have been inferred to start with a GGGG sequence [40], but their exact 5' end sequence is not formally demonstrated. Therefore, the methylation of such

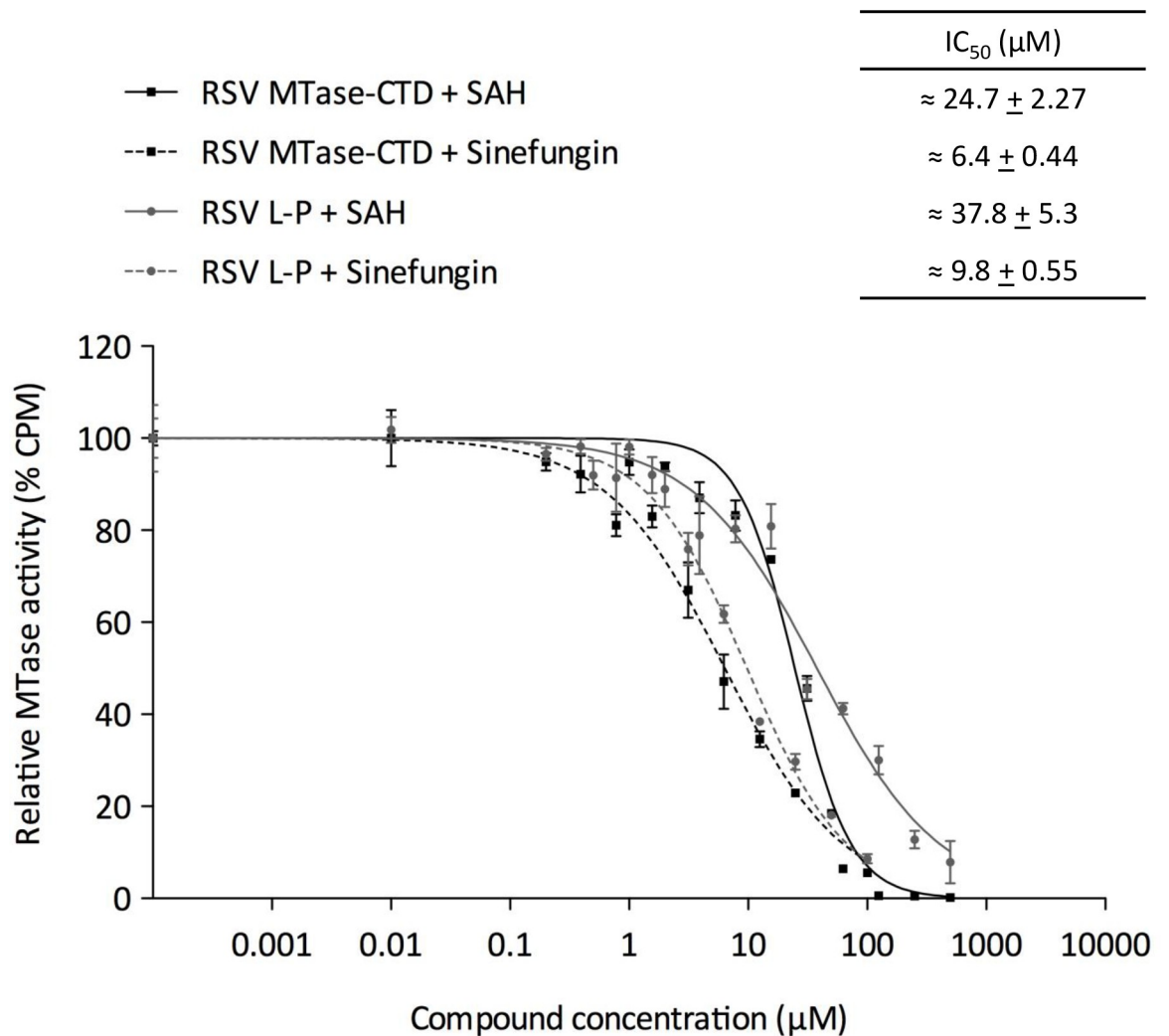


Fig 7. Inhibition of the MTase activity by SAM analogues. Increasing concentrations of SAH or sinefungin (previously dissolved in water) were incubated with 25 nM RSV MTase-CTD in a reaction mixture (40 mM Tris-HCl, pH 7.5, 2 μM SAM and 0.1 μM ³H-SAM) in the presence of 0.7 μM of GpppG-RSV₉ synthetic RNA, and with 60 nM RSV L-P complex in a reaction mixture (40 mM Tris-HCl, pH 7.5, 0.17 μM SAM and 0.8 μM ³H-SAM) in the presence of 1.8 μM synthetic RNA (GpppG-RSV₉). Reactions were incubated at 30 °C for 3 h. Values were normalized and fitted with Prism (GraphPad software) using the following equation: $Y = 100 / (1 + ((X/IC_{50})^{Hillslope}))$ (n = 3; mean value ± SEM).

<https://doi.org/10.1371/journal.ppat.1009562.g007>

RNAs might occur co-transcriptionally, on the nascent viral RNA synthesized by the RdRp domain of the L protein, to ensure their efficient methylation. The sequence specificity of the RSV MTase domain is also reflected by its low methylation activity in the presence of RNAs starting with sequences that mimic the 5' end of other viruses (coronavirus, filovirus, rhabdovirus and flavivirus). These findings suggest that the RSV MTase has a specific recognition mechanism based on the nucleotide sequence present at the 5' end of capped RSV RNA.

We also investigated whether the RSV MTase catalyzes only the specific methylation of cap structures or also additional internal RNA methylation, as previously reported for Ebola and flaviviruses (Dengue, Zika) [13,33,43,44]. We could barely detect the RSV MTase-CTD enzymatic activity in the presence of homo- and hetero-polymeric uncapped RNA substrates, as well as of ^mGpppG_m-RSV₉-RNA, suggesting that no internal methylation occurs in our

experimental conditions. This is strikingly different from what reported for the Ebola SUDV MTase that displays mainly internal methylation activity *in vitro* [33], and for the hMPV and Ebola virus MTases that catalyze the 2'-O-methylation of the first ribose nucleotide in the absence of any cap structure [34]. Thus, the cap or RNA recognition mechanism might be specific for the different NNS MTases that share a conserved MTase domain, but that have a CTD (involved in RNA recognition) of different length and sequence. Although the hMPV MTase CTD structure revealed that this MTase lacks any obvious cap-binding site [34], such as the one present in flaviviruses, coronaviruses and vaccinia virus [24,45,46], the RSV CTD might have evolved to accommodate preferentially cap structures. Additional studies are needed to determine the molecular bases of cap recognition by the RSV L protein.

Concerning the cap-dependent MTase activity, we characterized how the cap structure is methylated in our *in vitro* assay. Methyl transfer to RNA substrates that mimic the conserved start sequence of RSV 5' transcripts occurred at the 2'-O position and also N7 position in the FBA assay, but N7 methylation was catalyzed more efficiently in the time-course assay performed with the MTase-CTD construct. We obtained similar results (*i.e.* higher N7 MTase activity) also when we tested the RSV MTase in the context of the L-P complex. Nevertheless, we observed that the kinetics of methylation by the MTase in the L-P complex are slower compared to the MTase-CTD protein. This suggests that the accessibility of the MTase domain active site is decreased in the L-P complex. In these experimental conditions, N7-methylation occurred first, and 2'-O activity was only visible after overnight incubation. The time-course analysis of cap structure methylation by RSV MTase-CTD confirmed that there is a preferred sequence of methylation events. Altogether, these results suggest that N7-methylation occurs before the first RNA nucleotide (N1) 2'-O-methylation. This order of methylation events is different from what is described for the cap methylation mechanism of most mononegaviruses (VSV, hMPV, Ebola virus) in which 2'-O-methylation was proposed to precede N7 methylation [31–34,47]. Conversely, this mechanism is reminiscent of what is observed in eukaryotes (metazoans) and other viral systems, such as vaccinia virus [48–51], where the guanosine from the cap structure is methylated at the N7 position before methylation at the 2'-O position of N1 [52–55]. Regardless of the methylation sequence, the currently available mononegavirus structures suggests that the MTase domain possesses an active center (K-D-K-E) and a single SAM binding pocket involved in the methyl transfer reaction to two distinct acceptor positions with different chemical characteristics and conformational contexts. To achieve this, the mRNA cap substrate must accommodate two different positions: one with the guanine-N7 position and the other with the nucleoside-2'-O position facing the SAM methyl group [56,57].

In conclusion, this work shows that RSV harbors a SAM-dependent MTase activity to catalyze N7- and 2'-O-methylations of viral mRNA. Inhibition of such activities could limit viral replication and stimulate the antiviral response. We demonstrated that SAM analogues, such as sinefungin, inhibit the RSV MTase enzymatic activity of the L-P complex and of the MTase-CTD domain with similar IC₅₀ values. The biochemical characterization and enzymatic assays developed in this work pave the way for the development of new antiviral strategies to target the RSV MTase in order to limit the viral replication or potentiate the host antiviral response.

Materials and methods

Cloning and expression

The codon-optimized RSV MTase-CTD synthetic gene (Genscript) was cloned in a modified pGEX-4T-3 vector with an N-terminal 6x His-tag for bacterial expression. Mutants were generated by PCR amplification using the *Pfu* DNA polymerase kit (Promega) and primers carrying the mutations (S2 Table). Proteins were produced in *Escherichia coli* chaperone competent

pGro7/BL21 cells (Takara). Cells were grown in Luria broth with L-arabinose (1 g/L) at 30°C until the OD₆₀₀ value reached 0.6. Protein expression was induced with 20 μM IPTG at 16°C, overnight. Bacteria were then spun down (8000 rpm, 4°C, 10 min) using a Sorval Lynx 6000 centrifuge (Thermo Scientific), and pellets were stored at -80°C.

Protein purification

The MTase-CTD construct was purified as follows. Cell pellets from 1 L bacterial culture were resuspended in 30 ml lysis buffer (50 mM Tris-HCl pH 7.5, 500 mM NaCl, 20 mM imidazole, 10% glycerol, 2 mM PMSF, 2 mM β-mercaptoethanol, 1x BugBuster (Merck; 10x solution), 1% Triton X-100, 10 μg/mL DNase I, 0.25 mg/mL lysozyme, 1 tablet antiprotease cocktail (Bimake)), incubated at 4°C for 30 min, and sonicated. After cell lysate clarification (20,000 rpm, 4°C, 30 min), the supernatant was incubated with CoNTA resin (Thermo Scientific; 0.5 mL/L culture) at 4°C with gentle shaking for 1 h. Beads were transferred to a 25 mL column and washed with 2x10 mL of the following washing (W) buffers: W1 (50 mM Tris-HCl pH 7.5, 1 M NaCl, 20 mM imidazole, 10% glycerol, 1% Triton X-100, 2 mM β-mercaptoethanol), W2 (50 mM Tris-HCl pH 7.5, 50 mM NaCl, 20 mM imidazole, 10% glycerol, 1% Triton X-100, 2 mM β-mercaptoethanol), and W3 (50 mM Tris-HCl pH 7.5, 500 mM NaCl, 20 mM imidazole, 10% glycerol, 2 mM β-mercaptoethanol). Proteins were eluted with W3 buffer containing 250 mM imidazole and dialyzed overnight in heparin buffer A (20 mM Tris-HCl pH 7.5, 200 mM NaCl, 10% glycerol, 1 mM DTT). A HiTrap heparin column (GE Healthcare) was used as second purification step, and proteins were eluted with a linear gradient of heparin buffer B (20 mM Tris-HCl pH 7.5, 1.5 M NaCl, 10% glycerol, 1 mM DTT). Size-exclusion chromatography (SEC) was used as third purification step with a Superdex 200 10/300 GL column (GE Healthcare) in SEC buffer (50 mM Tris-HCl pH 7.5, 500 mM NaCl, 10% glycerol, 1 mM DTT). The RSV MTase-CTD was concentrated using Vivaspin ultrafiltration units (Sartorius), and stored at -20°C in SEC buffer containing 40% glycerol. Contrary to the hMPV and Ebola MTases that were purified in presence of arginine to increase their solubility, the RSV MTase was soluble in absence of arginine.

The L-P construct was produced and purified as previously described [35]. Briefly, the human RSV L protein (strain A2) with an N-terminal dual StrepTag and the RSV P protein (strain A2) with a C-terminal 6x His-tag were co-expressed in Sf9 insect cells using the pFAST-bac Dual transfer vector. The L-P complex was purified with two affinity chromatography steps, followed by size-exclusion chromatography [35].

MTase activity assay

The MTase activity was measured using a filter-binding assay, performed by combining 25 nM of RSV MTase-CTD with 0.7 μM of synthetic RNAs, 2 μM SAM, and 0.33 μM ³H-SAM (Perkin Elmer) in 40 mM Tris-HCl pH 7.5. After 3-h incubation at 30°C, reactions were quenched by 10-fold dilution in ice-cold 100 μM SAH, and samples were transferred to DEAE filtermats (Perkin Elmer) using a Filtermat Harvester (Packard Instruments). The RNA-retaining mats were washed twice with 10 mM ammonium formate (pH 8.0), twice with water, and once with ethanol. They were then soaked with liquid scintillation fluid for measuring ³H-methyl transfer to the RNA substrates using a Wallac MicroBeta TriLux Liquid Scintillation Counter (Perkin Elmer).

Synthesis of RNA substrates

RNA sequences were chemically synthesized on a solid support using an ABI 394 automated synthesizer with 2'-O-pivaloyloxymethyl 3'-O-phosphoramidite ribonucleosides and 2'-O-

methyl 3'-O-phosphoramidite guanosine (ChemGenes Corp., USA) [58]. After RNA assembly, the 5'-hydroxyl group was phosphorylated and the resulting *H*-phosphonate derivative was oxidized and activated into a phosphoroimidazolidate derivative to react with pyrophosphate [59] or GDP, giving pppRNA or GpppRNA, respectively. After deprotection and release from the solid support, RNA substrates were purified by IEX-HPLC (>95% pure) and their identity was confirmed by MALDI-TOF spectrometry. N7-methylation of the cap structure was performed using human (guanine-N7)-MTase [60].

Thin-layer chromatography (TLC) analysis of cap structures

Radioactive capped G*ppp RNAs (in which the asterisk indicates the [³²P]-labelled phosphate) were synthesized by incubating ppp RNA (10 μM) with the vaccinia virus capping enzyme (New England Biolabs) in the presence of 1.65 μCi [α-³²P]-GTP (Perkin Elmer). Capped RNAs were purified with MicroSpin G-25 columns (GE Healthcare) and StrataClean resin (Agilent) before incubation with the RSV MTase-CTD. After methylation, capped RNAs were purified by precipitation in 3 M sodium acetate supplemented with 1 μg μL⁻¹ of glycogen (Thermo Scientific), followed by digestion with 1 U of nuclease P1 (Sigma) at 37°C for 1 h. Digested products were spotted onto polyethylenimine cellulose TLC plates (Macherey Nagel), and resolved using 0.65 M LiCl as mobile phase. After autoradiography, the radiolabeled caps released by the nuclease P1 were visualized using an Amersham Typhoon Biomolecular Imager (GE Healthcare). The quantitative analysis was performed using the ImageQuant TL software (GE Healthcare). The initial velocity was determined by linear regression analysis of the linear phase of a product build-up using GraphPad Prism version 5.0.

Supporting information

S1 Fig. Mutagenesis of the RSV MTase-CTD protein and effect on N7- and 2'-O-methylation. (A) Amino acid sequence alignment of the C-terminal portion of the indicated L proteins showing the amino acid residues of the catalytic tetrad (K-D-K-E) and the amino acid residues thought to participate in SAM and RNA-binding that were mutated. The amino acid sequences of the L protein from RSV strain A2 (P28887), human metapneumovirus (Q91L20), Zaire ebolavirus strain Mayinga-76 (Q05318) and vesicular stomatitis virus Indiana strain (P03523.2) were aligned using Seaview (Gouy *et al.*, 2010) and ESPript (<http://espript.ibcp.fr>) (Robert *et al.*, 2014). (B) SDS-PAGE of wild-type (WT) RSV MTase-CTD and mutant proteins (that were successfully expressed) after Coomassie blue staining, purified by affinity chromatography. Molecular weights (in kilodaltons) are shown on the left. (C) The effect of point mutations (see panel A) in the RSV MTase-CTD on the MTase activity was analyzed by filter-binding assay. Samples were purified by affinity chromatography. GpppG-RSV₉ was used as substrate and the RSV MTase-CTD was used at 25 nM. Data are the mean ± SEM of three independent measurements. (TIF)

S2 Fig. MTase activity reaction optimization. (A) Methylation activity of the RSV MTase-CTD protein measured by filter-binding assay using GpppG-RSV₉ RNA as template at different pH (from 6.0 to 9.0). Plotted values were obtained after 3 h incubation at 30°C. The RSV MTase-CTD was used at the concentration of 25 nM. Data are the mean ± SEM of three independent measurements. (B) Methylation activity of the RSV MTase-CTD protein (25 nM) measured as in (A) in the standard reaction buffer (50 mM Tris-HCl; pH 8.0) or with different additives. Plotted values were obtained after 4 h incubation at 30°C. Data are the mean ± SEM

of three independent measurements.
(TIF)

S3 Fig. Inhibition of the MTase activity by cap analogues. Increasing concentrations of (A) unmethylated (Gppp A, Gppp G) and (B) N7-methylated (^mGppp A, ^mGDP) cap analogues (previously dissolved in water) were incubated with 25 nM RSV MTase-CTD in a reaction mixture (40 mM Tris-HCl, pH 7.5, 2 μM SAM and 0.1 μM ³H-SAM) in the presence of 0.7 μM of GpppG-RSV₉ synthetic RNA. Reactions were incubated at 30°C for 3 h. Values were normalized and fitted with GraphPad Prism version 5.0 using the following equation: $Y = 100 / (1 + ((X/IC_{50})^{Hillslope}))$ (n = 3; mean value ± SEM).
(TIF)

S1 Table. Liste of synthetic RNAs. Unmethylated caps are denoted by ‘Gppp’, N7-methylated caps by ‘mGppp’, 2'-O-methylated residues by ‘Xm’. Full-length sequences can be found in the second column, manufacturing information in the third one.
(TIF)

S2 Table. Liste of primers. Primers were used for site-directed mutagenesis of RSV MTase-CTD protein by PCR amplification using the Pfu DNA polymerase kit (Promega).
(TIF)

Acknowledgments

The authors wish to thank Drs Zhinan Jin and Cheng Liu for providing RSV L-P expression plasmids and expert advice on protein expression and purification. We thank Barbara Selisko for her scientific contributions.

Author Contributions

Conceptualization: Priscila Sutto-Ortiz, Nina Ysebaert, Dirk Roymans, Peter Rigaux, Jean-François Eléouët, Etienne Decroly.

Data curation: Priscila Sutto-Ortiz, Etienne Decroly.

Formal analysis: Priscila Sutto-Ortiz, Etienne Decroly.

Funding acquisition: Dirk Roymans, Peter Rigaux, Jean-François Eléouët, Etienne Decroly.

Investigation: Priscila Sutto-Ortiz, Sergey Tcherniuk, Jean-François Eléouët, Etienne Decroly.

Methodology: Priscila Sutto-Ortiz, Sergey Tcherniuk, Pravién Abeywickrema, Mathieu Noël, Alice Decombe, Françoise Debart, Jean-Jacques Vasseur, Jean-François Eléouët, Etienne Decroly.

Project administration: Dirk Roymans, Peter Rigaux, Etienne Decroly.

Resources: Dirk Roymans, Peter Rigaux, Etienne Decroly.

Supervision: Dirk Roymans, Peter Rigaux, Etienne Decroly.

Validation: Bruno Canard, Dirk Roymans, Peter Rigaux, Etienne Decroly.

Visualization: Jean-François Eléouët, Etienne Decroly.

Writing – original draft: Priscila Sutto-Ortiz, Etienne Decroly.

Writing – review & editing: Priscila Sutto-Ortiz, Sergey Tcherniuk, Nina Ysebaert, Pravien Abeywickrema, Mathieu Noël, Alice Decombe, Françoise Debart, Jean-Jacques Vasseur, Bruno Canard, Dirk Roymans, Peter Rigaux, Jean-François Eléouët, Etienne Decroly.

References

1. Glezen WP, Taber LH, Frank AL, Kasel JA. Risk of primary infection and reinfection with respiratory syncytial virus. *Am J Dis Child*. 1986; 140(6):543–6. Epub 1986/06/01. <https://doi.org/10.1001/archpedi.1986.02140200053026> PMID: 3706232.
2. Shi T, McAllister DA, O'Brien KL, Simoes EAF, Madhi SA, Gessner BD, et al. Global, regional, and national disease burden estimates of acute lower respiratory infections due to respiratory syncytial virus in young children in 2015: a systematic review and modelling study. *Lancet*. 2017; 390(10098):946–58. Epub 2017/07/12. S0140-6736(17)30938-8 [pii] [https://doi.org/10.1016/S0140-6736\(17\)30938-8](https://doi.org/10.1016/S0140-6736(17)30938-8) PMID: 28689664.
3. Falsey AR, Hennessey PA, Formica MA, Cox C, Walsh EE. Respiratory syncytial virus infection in elderly and high-risk adults. *N Engl J Med*. 2005; 352(17):1749–59. Epub 2005/04/29. <https://doi.org/10.1056/NEJMoa043951> PMID: 15858184.
4. Shahabi A, Peneva D, Incerti D, McLaurin K, Stevens W. Assessing Variation in the Cost of Palivizumab for Respiratory Syncytial Virus Prevention in Preterm Infants. *Pharmacoecon Open*. 2017; 2(1):53–61. Epub 2018/02/22. <https://doi.org/10.1007/s41669-017-0042-3> [pii] 42 [pii]10.1007/s41669-017-0042-3 [doi]. PMID: 29464672.
5. Homaira N, Rawlinson W, Snelling TL, Jaffe A. Effectiveness of Palivizumab in Preventing RSV Hospitalization in High Risk Children: A Real-World Perspective. *Int J Pediatr*. 2014; 2014:571609. Epub 2014/12/31. <https://doi.org/10.1155/2014/571609> PMID: 25548575.
6. Battles MB, McLellan JS. Respiratory syncytial virus entry and how to block it. *Nat Rev Microbiol*. 2019; 17(4):233–45. Epub 2019/02/07. <https://doi.org/10.1038/s41579-019-0149-x> [pii]149 [pii]10.1038/s41579-019-0149-x [doi]. PMID: 30723301.
7. Amarasinghe GK, Arechiga Ceballos NG, Banyard AC, Basler CF, Bavari S, Bennett AJ, et al. Taxonomy of the order Mononegavirales: update 2018. *Arch Virol*. 2018; 163(8):2283–94. Epub 2018/04/11. <https://doi.org/10.1007/s00705-018-3814-x> [doi]10.1007/s00705-018-3814-x [pii]. PMID: 29637429.
8. Grosfeld H, Hill MG, Collins PL. RNA replication by respiratory syncytial virus (RSV) is directed by the N, P, and L proteins; transcription also occurs under these conditions but requires RSV superinfection for efficient synthesis of full-length mRNA. *J Virol*. 1995; 69(9):5677–86. Epub 1995/09/01. <https://doi.org/10.1128/JVI.69.9.5677-5686.1995> PMID: 7637014.
9. Yu Q, Hardy RW, Wertz GW. Functional cDNA clones of the human respiratory syncytial (RS) virus N, P, and L proteins support replication of RS virus genomic RNA analogs and define minimal trans-acting requirements for RNA replication. *J Virol*. 1995; 69(4):2412–9. Epub 1995/04/01. <https://doi.org/10.1128/JVI.69.4.2412-2419.1995> PMID: 7884888.
10. Collins PL, Hill MG, Camargo E, Grosfeld H, Chanock RM, Murphy BR. Production of infectious human respiratory syncytial virus from cloned cDNA confirms an essential role for the transcription elongation factor from the 5' proximal open reading frame of the M2 mRNA in gene expression and provides a capability for vaccine development. *Proc Natl Acad Sci U S A*. 1995; 92(25):11563–7. Epub 1995/12/05. <https://doi.org/10.1073/pnas.92.25.11563> PMID: 8524804.
11. Bakker SE, Duquerroy S, Galloux M, Loney C, Conner E, Eleouet JF, et al. The respiratory syncytial virus nucleoprotein-RNA complex forms a left-handed helical nucleocapsid. *J Gen Virol*. 2013; 94(Pt 8):1734–8. Epub 2013/05/17. <https://doi.org/10.1099/vir.0.053025-0> PMID: 23677789.
12. Tawar RG, Duquerroy S, Vonrhein C, Varela PF, Damier-Piolle L, Castagne N, et al. Crystal structure of a nucleocapsid-like nucleoprotein-RNA complex of respiratory syncytial virus. *Science*. 2009; 326(5957):1279–83. Epub 2009/12/08. 326/5957/1279 [pii] <https://doi.org/10.1126/science.1177634> PMID: 19965480.
13. Valle C, Martin B, Debart F, Vasseur JJ, Imbert I, Canard B, et al. The C-Terminal Domain of the Sudan Ebolavirus L Protein Is Essential for RNA Binding and Methylation. *J Virol*. 2020; 94(12). Epub 2020/04/10. JVI.00520-20 [pii] 00520–20 [pii] <https://doi.org/10.1128/JVI.00520-20> PMID: 32269120.
14. Galloux M, Tarus B, Blazevic I, Fix J, Duquerroy S, Eleouet JF. Characterization of a viral phosphoprotein binding site on the surface of the respiratory syncytial nucleoprotein. *J Virol*. 2012; 86(16):8375–87. Epub 2012/05/25. JVI.00058-12 [pii] <https://doi.org/10.1128/JVI.00058-12> PMID: 22623798.
15. Tran TL, Castagne N, Bhella D, Varela PF, Bernard J, Chilmonczyk S, et al. The nine C-terminal amino acids of the respiratory syncytial virus protein P are necessary and sufficient for binding to ribonucleoprotein complexes in which six ribonucleotides are contacted per N protein protomer. *J Gen Virol*. 2007; 88(Pt 1):196–206. Epub 2006/12/16. <https://doi.org/10.1099/vir.0.82282-0> PMID: 17170452.

16. Shatkin AJ. Capping of eucaryotic mRNAs. *Cell*. 1976; 9(4 PT 2):645–53. Epub 1976/12/01. 0092-8674 (76)90128-8 [pii] [https://doi.org/10.1016/0092-8674\(76\)90128-8](https://doi.org/10.1016/0092-8674(76)90128-8) PMID: 1017010.
17. Filipowicz W, Furuichi Y, Sierra JM, Muthukrishnan S, Shatkin AJ, Ochoa S. A protein binding the methylated 5'-terminal sequence, m7GpppN, of eukaryotic messenger RNA. *Proc Natl Acad Sci U S A*. 1976; 73(5):1559–63. Epub 1976/05/01. <https://doi.org/10.1073/pnas.73.5.1559> PMID: 1064023.
18. Schibler U, Perry RP. The 5'-termini of heterogeneous nuclear RNA: a comparison among molecules of different sizes and ages. *Nucleic Acids Res*. 1977; 4(12):4133–49. Epub 1977/12/01. <https://doi.org/10.1093/nar/4.12.4133> PMID: 600792.
19. Darnell JE Jr. Transcription units for mRNA production in eukaryotic cells and their DNA viruses. *Prog Nucleic Acid Res Mol Biol*. 1979; 22:327–53. Epub 1979/01/01. [https://doi.org/10.1016/s0079-6603\(08\)60803-x](https://doi.org/10.1016/s0079-6603(08)60803-x) PMID: 523634.
20. Devarkar SC, Wang C, Miller MT, Ramanathan A, Jiang F, Khan AG, et al. Structural basis for m7G recognition and 2'-O-methyl discrimination in capped RNAs by the innate immune receptor RIG-I. *Proc Natl Acad Sci U S A*. 2016; 113(3):596–601. Epub 2016/01/07. 1515152113 [pii] <https://doi.org/10.1073/pnas.1515152113> PMID: 26733676.
21. Nallagatla SR, Toroney R, Bevilacqua PC. A brilliant disguise for self RNA: 5'-end and internal modifications of primary transcripts suppress elements of innate immunity. *RNA Biol*. 2008; 5(3):140–4. Epub 2008/09/05. 6839 [pii] <https://doi.org/10.4161/ra.5.3.6839> PMID: 18769134.
22. Rehwinkel J, Tan CP, Goubau D, Schulz O, Pichlmair A, Bier K, et al. RIG-I detects viral genomic RNA during negative-strand RNA virus infection. *Cell*. 2010; 140(3):397–408. Epub 2010/02/11. S0092-8674 (10)00021-8 [pii] <https://doi.org/10.1016/j.cell.2010.01.020> PMID: 20144762.
23. Decroly E, Canard B. Biochemical principles and inhibitors to interfere with viral capping pathways. *Curr Opin Virol*. 2017; 24:87–96. Epub 2017/05/22. S1879-6257(17)30019-6 [pii] <https://doi.org/10.1016/j.coviro.2017.04.003> PMID: 28527860.
24. Decroly E, Ferron F, Lescar J, Canard B. Conventional and unconventional mechanisms for capping viral mRNA. *Nat Rev Microbiol*. 2011; 10(1):51–65. Epub 2011/12/06. nrmicro2675 [pii] <https://doi.org/10.1038/nrmicro2675> PMID: 22138959.
25. Ma Y, Wei Y, Zhang X, Zhang Y, Cai H, Zhu Y, et al. mRNA cap methylation influences pathogenesis of vesicular stomatitis virus in vivo. *J Virol*. 2014; 88(5):2913–26. Epub 2013/12/29. JVI.03420-13 [pii] <https://doi.org/10.1128/JVI.03420-13> PMID: 24371058.
26. Zhang Y, Wei Y, Zhang X, Cai H, Niewiesk S, Li J. Rational design of human metapneumovirus live attenuated vaccine candidates by inhibiting viral mRNA cap methyltransferase. *J Virol*. 2014; 88(19):11411–29. Epub 2014/07/25. JVI.00876-14 [pii]00876–14 [pii] <https://doi.org/10.1128/JVI.00876-14> PMID: 25056882.
27. Li J, Rahmeh A, Brusich V, Whelan SP. Opposing effects of inhibiting cap addition and cap methylation on polyadenylation during vesicular stomatitis virus mRNA synthesis. *J Virol*. 2009; 83(4):1930–40. Epub 2008/12/17. JVI.02162-08 [pii] <https://doi.org/10.1128/JVI.02162-08> PMID: 19073725.
28. Abraham G, Rhodes DP, Banerjee AK. The 5' terminal structure of the methylated mRNA synthesized in vitro by vesicular stomatitis virus. *Cell*. 1975; 5(1):51–8. Epub 1975/05/01. 0092-8674(75)90091-4 [pii] [https://doi.org/10.1016/0092-8674\(75\)90091-4](https://doi.org/10.1016/0092-8674(75)90091-4) PMID: 165900.
29. Barik S. The structure of the 5' terminal cap of the respiratory syncytial virus mRNA. *J Gen Virol*. 1993; 74 (Pt 3):485–90. Epub 1993/03/01. <https://doi.org/10.1099/0022-1317-74-3-485> PMID: 8445369.
30. Gupta KC, Roy P. Alternate capping mechanisms for transcription of spring viremia of carp virus: evidence for independent mRNA initiation. *J Virol*. 1980; 33(1):292–303. Epub 1980/01/01. <https://doi.org/10.1128/JVI.33.1.292-303.1980> PMID: 16789187.
31. Ogino T, Banerjee AK. Unconventional mechanism of mRNA capping by the RNA-dependent RNA polymerase of vesicular stomatitis virus. *Mol Cell*. 2007; 25(1):85–97. Epub 2007/01/16. S1097-2765 (06)00785-4 [pii] <https://doi.org/10.1016/j.molcel.2006.11.013> PMID: 17218273.
32. Rahmeh AA, Li J, Kranzusch PJ, Whelan SP. Ribose 2'-O methylation of the vesicular stomatitis virus mRNA cap precedes and facilitates subsequent guanine-N-7 methylation by the large polymerase protein. *J Virol*. 2009; 83(21):11043–50. Epub 2009/08/28. JVI.01426-09 [pii]1426–09 [pii] <https://doi.org/10.1128/JVI.01426-09> PMID: 19710136.
33. Martin B, Coutard B, Guez T, Paesen GC, Canard B, Debart F, et al. The methyltransferase domain of the Sudan ebolavirus L protein specifically targets internal adenosines of RNA substrates, in addition to the cap structure. *Nucleic Acids Res*. 2018; 46(15):7902–12. Epub 2018/09/08. 5052367 [pii] <https://doi.org/10.1093/nar/gky637> PMID: 30192980.
34. Paesen GC, Collet A, Sallamand C, Debart Fo, Vasseur J-J, Canard B, et al. X-ray structure and activities of an essential Mononegavirales L-protein domain. *Nature Comm*. 2015; 6(1):8749. <https://doi.org/10.1038/ncomms9749> Paesen2015. PMID: 26549102

35. Gilman MSA, Liu C, Fung A, Behera I, Jordan P, Rigaux P, et al. Structure of the Respiratory Syncytial Virus Polymerase Complex. *Cell*. 2019; 179(1):193–204 e14. Epub 2019/09/10. S0092-8674(19)30902-X [pii] <https://doi.org/10.1016/j.cell.2019.08.014> PMID: 31495574.
36. Jenni S, Bloyet LM, Diaz-Avalos R, Liang B, Whelan SPJ, Grigorieff N, et al. Structure of the Vesicular Stomatitis Virus L Protein in Complex with Its Phosphoprotein Cofactor. *Cell Rep*. 2020; 30(1):53–60 e5. Epub 2020/01/09. S2211-1247(19)31674-2 [pii] <https://doi.org/10.1016/j.celrep.2019.12.024> PMID: 31914397.
37. Liang B, Li Z, Jenni S, Rahmeh AA, Morin BM, Grant T, et al. Structure of the L Protein of Vesicular Stomatitis Virus from Electron Cryomicroscopy. *Cell*. 2015; 162(2):314–27. Epub 2015/07/07. S0092-8674(15)00702-3 [pii] <https://doi.org/10.1016/j.cell.2015.06.018> PMID: 26144317.
38. Stec DS, Hill MG, 3rd, Collins PL. Sequence analysis of the polymerase L gene of human respiratory syncytial virus and predicted phylogeny of nonsegmented negative-strand viruses. *Virology*. 1991; 183(1):273–87. Epub 1991/07/01. [https://doi.org/10.1016/0042-6822\(91\)90140-7](https://doi.org/10.1016/0042-6822(91)90140-7) PMID: 2053282
39. Collins PL, Huang YT, Wertz GW. Nucleotide sequence of the gene encoding the fusion (F) glycoprotein of human respiratory syncytial virus. *Proc Natl Acad Sci U S A*. 1984; 81(24):7683–7. Epub 1984/12/01. <https://doi.org/10.1073/pnas.81.24.7683> PMID: 6096849.
40. Johnson PR, Collins PL. The 1B (NS2), 1C (NS1) and N proteins of human respiratory syncytial virus (RSV) of antigenic subgroups A and B: sequence conservation and divergence within RSV genomic RNA. *J Gen Virol*. 1989; 70 (Pt 6):1539–47. Epub 1989/06/01. <https://doi.org/10.1099/0022-1317-70-6-1539> PMID: 2525176.
41. Li J, Chorba JS, Whelan SP. Vesicular stomatitis viruses resistant to the methylase inhibitor sinefungin upregulate RNA synthesis and reveal mutations that affect mRNA cap methylation. *J Virol*. 2007; 81(8):4104–15. Epub 2007/02/16. JVI.02681-06 [pii]2681–06 [pii] <https://doi.org/10.1128/JVI.02681-06> PMID: 17301155.
42. Dochow M, Krumm SA, Crowe JE Jr., Moore ML, Plemper RK. Independent structural domains in paramyxovirus polymerase protein. *J Biol Chem*. 2012; 287(9):6878–91. Epub 2012/01/05. S0021-9258(20)61170-X [pii]M111.325258 [pii] <https://doi.org/10.1074/jbc.M111.325258> PMID: 22215662.
43. Coutard B, Barral K, Lichiere J, Selisko B, Martin B, Aouadi W, et al. Zika Virus Methyltransferase: Structure and Functions for Drug Design Perspectives. *J Virol*. 2017; 91(5). Epub 2016/12/30. JVI.02202-16 [pii] <https://doi.org/10.1128/JVI.02202-16> PMID: 28031359.
44. Dong H, Chang DC, Hua MH, Lim SP, Chionh YH, Hia F, et al. 2'-O methylation of internal adenosine by flavivirus NS5 methyltransferase. *PLoS Pathog*. 2012; 8(4):e1002642. Epub 2012/04/13. PPATHOGENS-D-11-01974 [pii] <https://doi.org/10.1371/journal.ppat.1002642> PMID: 22496660.
45. Egloff MP, Decroly E, Malet H, Selisko B, Benarroch D, Ferron F, et al. Structural and functional analysis of methylation and 5'-RNA sequence requirements of short capped RNAs by the methyltransferase domain of dengue virus NS5. *J Mol Biol*. 2007; 372(3):723–36. Epub 2007/08/10. S0022-2836(07)00914-X [pii] <https://doi.org/10.1016/j.jmb.2007.07.005> PMID: 17686489.
46. Hu G, Oguro A, Li C, Gershon PD, Quioco FA. The "cap-binding slot" of an mRNA cap-binding protein: quantitative effects of aromatic side chain choice in the double-stacking sandwich with cap. *Biochemistry*. 2002; 41(24):7677–87. Epub 2002/06/12. <https://doi.org/10.1021/bi0201926> [pii]10.1021/bi0201926 [doi]. PMID: 12056899.
47. Testa D, Banerjee AK. Two methyltransferase activities in the purified virions of vesicular stomatitis virus. *J Virol*. 1977; 24(3):786–93. Epub 1977/12/01. <https://doi.org/10.1128/JVI.24.3.786-793.1977> PMID: 201777.
48. Barbosa E, Moss B. mRNA(nucleoside-2'-)-methyltransferase from vaccinia virus. Purification and physical properties. *J Biol Chem*. 1978; 253(21):7692–7. Epub 1978/11/10. PMID: 701281.
49. Ensinger MJ, Martin SA, Paoletti E, Moss B. Modification of the 5'-terminus of mRNA by soluble guanylyl and methyl transferases from vaccinia virus. *Proc Natl Acad Sci U S A*. 1975; 72(7):2525–9. Epub 1975/07/01. <https://doi.org/10.1073/pnas.72.7.2525> PMID: 1058472.
50. Martin SA, Moss B. Modification of RNA by mRNA guanylyltransferase and mRNA (guanine-7-)methyltransferase from vaccinia virions. *J Biol Chem*. 1975; 250(24):9330–5. Epub 1975/12/25. PMID: 1194287.
51. Martin SA, Moss B. mRNA guanylyltransferase and mRNA (guanine-7-)methyltransferase from vaccinia virions. Donor and acceptor substrate specificities. *J Biol Chem*. 1976; 251(23):7313–21. Epub 1976/12/10. PMID: 1002690.
52. Langberg SR, Moss B. Post-transcriptional modifications of mRNA. Purification and characterization of cap I and cap II RNA (nucleoside-2'-)-methyltransferases from HeLa cells. *J Biol Chem*. 1981; 256(19):10054–60. Epub 1981/10/10. PMID: 7275966.

53. Mizumoto K, Lipmann F. Transmethylation and transguanylylation in 5'-RNA capping system isolated from rat liver nuclei. *Proc Natl Acad Sci U S A*. 1979; 76(10):4961–5. Epub 1979/10/01. <https://doi.org/10.1073/pnas.76.10.4961> PMID: 291913.
54. Ogino T, Banerjee AK. An unconventional pathway of mRNA cap formation by vesiculoviruses. *Virus Res*. 2011; 162(1–2):100–9. Epub 2011/09/29. S0168-1702(11)00349-2 [pii] <https://doi.org/10.1016/j.virusres.2011.09.012> PMID: 21945214.
55. Wei C, Moss B. 5'-Terminal capping of RNA by guanylyltransferase from HeLa cell nuclei. *Proc Natl Acad Sci U S A*. 1977; 74(9):3758–61. Epub 1977/09/01. <https://doi.org/10.1073/pnas.74.9.3758> PMID: 269428.
56. Dong H, Ren S, Zhang B, Zhou Y, Puig-Basagoiti F, Li H, et al. West Nile virus methyltransferase catalyzes two methylations of the viral RNA cap through a substrate-repositioning mechanism. *J Virol*. 2008; 82(9):4295–307. Epub 2008/02/29. JVI.02202-07 [pii]2202–07 [pii] <https://doi.org/10.1128/JVI.02202-07> PMID: 18305027.
57. Li J, Wang JT, Whelan SP. A unique strategy for mRNA cap methylation used by vesicular stomatitis virus. *Proc Natl Acad Sci U S A*. 2006; 103(22):8493–8. Epub 2006/05/20. 0509821103 [pii] <https://doi.org/10.1073/pnas.0509821103> PMID: 16709677.
58. Lavergne T, Bertrand JR, Vasseur JJ, Debart F. A base-labile group for 2'-OH protection of ribonucleosides: a major challenge for RNA synthesis. *Chem. Eur J*. 2008; 14(30):9135–8. Epub 2008/09/04. <https://doi.org/10.1002/chem.200801392> PMID: 18767078.
59. Zlatev I, Lavergne T, Debart F, Vasseur JJ, Manoharan M, Morvan F. Efficient solid-phase chemical synthesis of 5'-triphosphates of DNA, RNA, and their analogues. *Org Lett*. 2010; 12(10):2190–3. Epub 2010/04/28. <https://doi.org/10.1021/ol1004214> PMID: 20420425.
60. Thillier Y, Decroly E, Morvan F, Canard B, Vasseur JJ, Debart F. Synthesis of 5' cap-0 and cap-1 RNAs using solid-phase chemistry coupled with enzymatic methylation by human (guanine-N7)-methyl transferase. *RNA*. 2012; 18(4):856–68. Epub 2012/02/16. ma.030932.111 [pii]RA [pii] <https://doi.org/10.1261/ma.030932.111> PMID: 22334760.